Investigational New Drugs (2019) 37:865–875
https://doi.org/10.1007/s10637-018-0702-x

PRECLINICAL STUDIES

A mediator of phosphorylated Smad2/3, evodiamine, in the reversion of TAF-induced EMT in normal colonic epithelial cells

Wanbin Yang[1] · Xiuli Gong[2] · Xiulian Wang[3] · Chao Huang[4]

Received: 22 September 2018 / Accepted: 14 November 2018 / Published online: 29 November 2018

Summary

Purpose Transdifferentiation exists within stromal cells in the tumour microenvironment. Transforming growth factor-β (TGF-β) secreted by tumour-associated fibroblasts (TAFs) affects the differentiation states of epithelial cells, including epithelial-mesenchymal transition (EMT). Evodiamine, a natural drug, can regulate differentiation. However, the specific effects and relative mechanisms of evodiamine remain unknown. *Design* We used four models to observe the influence of TAF-like CCD-18Co cells on the colon epithelial cell line HCoEpiC: the 3D- and 2D-mono-culture system, Transwell and direct co-culture model. Additionally, we established conditioned medium from CCD-18Co cells. The TGF-β pathway inhibitor LY364947 and evodiamine were added. Morphological changes and classical EMT markers were observed and detected using phase contrast microscopy and immunofluorescence. Cell migration was measured by the wound-healing assay. Western blotting was performed to detect the TGF-β/Smad signalling pathway. *Results* CCD-18Co cells induced EMT-like changes in the 2D- and 3D-cultured epithelial cell line HCoEpiC, accompanied by high expression of ZEB1 and Snail and the enhancement of migration. Moreover, CCD-18Co-derived conditioned medium caused dysfunction of TGF-β/Smad signalling in EMT. Evodiamine inhibited these EMT-like HCoEpiC and their migration. Additionally, evodiamine down-regulated the expression of ZEB1/Snail and up-regulated the expression of phosphorylated Smad2/3 (pSmad2/3). Evodiamine also increased the ratios of pSmad2/Smad2 and pSmad3/Smad3. *Conclusion* Based on our observations, evodiamine can reverse the TAF-induced EMT-like phenotype in colon epithelial cells, which may be associated with its mediation of phosphorylated Smad2 and Smad3 expression.

Keywords Epithelial-mesenchymal transition · Tumour-associated fibroblasts · Tumour microenvironment · Transdifferentiation · Transforming growth factor-β · Evodiamine

✉ Chao Huang
huangchao06@163.com

[1] Institute of Tropical Diseases, Guangzhou University of Chinese Medicine, Guangzhou, Guangdong 510000, People's Republic of China

[2] Department of Spleen and Stomach Diseases, Second Hospital of Traditional Chinese Medicine of Guangdong, Guangzhou, Guangdong 510000, People's Republic of China

[3] Department of Traditional Chinese Medicine, Affiliated Bao'an Hospital of Traditional Chinese Medicine of Shenzhen, Guangzhou University of Chinese Medicine, Shenzhen, Guangdong 518000, People's Republic of China

[4] Central Laboratory, Affiliated Bao'an Hospital of Shenzhen, Southern Medical University, Shenzhen, Guangdong 518000, People's Republic of China

Introduction

Increasing evidence has indicated that the tumour microenvironment (TME) participates in tumourigenesis. The TME consists of various cell types, including endothelial cells, leukocytes, epithelial cells, fibroblasts and cancer cells, and complex communication networks exist between cancer cells and nearby stroma cells. These networks trigger diverse signalling pathways to stimulate cancer initiation and progression. As sentinel cells, normal fibroblasts play important functions in the maintenance of epithelial tissue homeostasis and prevention of the initiation of colon tumourigenesis. Unfortunately, fibroblasts existing in the TME or tumour stroma exhibit an activated and a myofibroblast-like phenotype with α-SMA expression. These fibroblasts are primary cell types within the stroma and are called cancer-associated fibroblasts

(CAFs) or tumour-associated fibroblasts (TAFs) [1]. These TAFs or CAFs promote cancer development and progression by offering cancer cells a myriad of cytokines and growth factors [1, 2]. Among these factors, transforming growth factor-β (TGF-β) is a major active cytokine [3]. TAF-derived TGF-β can act not only on tumour cells but also on host cells [4]. The interaction between tumour cells and stromal cells or between TAFs and other stromal cells promotes the generation of an optimal microenvironment, contributing to tumour development throughout all the steps of carcinogenesis at the microenvironment level [5].

However, TAFs in the TME can also communicate with other stroma cells, including epithelial cells. An established form of the communication is epithelial-mesenchymal transition (EMT) [6]. TAF-secreted TGF-β induces EMT-like phenotypes in epithelial cells. The epithelial cells undergoing phenotypic changes participate in the synthesis of the profibrotic matrix [7], which provides a pro-tumourigenic local niche for cancer growth. Therefore, pharmacological inhibition of the TGF-β/Smad pathway may be an effective and a promising therapy to suppress the pro-EMT transformation of epithelial cells.

Evodiamine (Evo), a natural product extracted from herbal plants such as Tetradium, has been applied to treat multiple diseases for centuries in China. Evo exerts multiple biological functions, including cytotoxicity [8], the inhibition of cell migration and invasion [9], and the induction of apoptosis. Emerging and increasing studies have focused on its anticancer functions through multiple mechanisms. However, the influence of Evo on TME is vague.

In the present study, we used a myofibroblast line CCD-18Co from the colon and extracted its culture supernatant called the conditioned medium. Next, the normal colon epithelial cell line HCoEpiC (2D model) was induced by the medium. Simultaneously, two other models, co-culture and 3-dimensional (3D) culture models, were established to observe the effect of CCD-18Co on HCoEpiC. Interestingly, the induction of EMT was indeed realized in the above models and was reversed by the TGF-β1 antagonist and Evo. Our findings may provide an innovation of Evo for anti-cancer treatment through regulating the TAF-induced phenotypic transition of normal colon epithelium.

Methods

Cell line origin and maintenance

The human normal colon epithelial cell line HCoEpiC from the American Type Culture Collection (ATCC) was purchased from GuangZhou Jennio Biotech Co., Ltd. (Guangzhou, Guangdong, China). CCD-18Co, a human colon myofibroblast line, was obtained from the ATCC.

HCoEpiC were recovered and cultured in RPMI 1640 (Gibco; 1830908) supplemented with 10% foetal bovine serum (FBS; 1861242; Gibco, USA), 2 g/L of $NaHCO_3$, and 1% penicillin/streptomycin (Solarbio, 20171222). The CCD-18Co cells were maintained in Dulbecco's modified Eagle's medium (DMEM) (8117280; Gibco) supplemented with 4.5 g/L of D-Glucose, 10% FBS and 1% penicillin/streptomycin. All the cells were cultured at 37 °C in a humidified atmosphere with 5% (*v*/v) CO_2.

Primary antibodies and reagents

Cultrex® Basement Membrane Extract (BME; PathClear®, Trevigen, Inc.; 3432–010-01) is a soluble form of the basement membrane purified from a Engelbreth-Holm-Swarm (EHS) tumour. The extract gels at 37 °C can form a reconstituted basement membrane. The major components of the BME include laminin, collagen IV, entactin, and heparin sulphate proteoglycan.

Evodiamine (Evo) and TGFβ receptor kinase I inhibitor LY364947 were purchased from Abcam (ab141890 and ab142427, respectively). The following primary antibodies were used: rabbit monoclonal anti-vimentin antibody (ab92547; Abcam), rabbit monoclonal anti-alpha smooth muscle actin (α-SMA) antibody (ab124964; Abcam), mouse monoclonal anti-E-cadherin antibody (AF0138; Beyotime Biotechnology, China), rabbit monoclonal anti-ZEB1 antibody (ab203829; Abcam), rabbit monoclonal anti-Snail antibody (ab216347; Abcam), rabbit monoclonal anti-Smad2 antibody (AF1300; Beyotime, China), rabbit monoclonal anti-Smad3 antibody (AF1501; Beyotime, China), rabbit monoclonal anti-phospho-Smad2 (Ser250) antibody (AF2545; Beyotime, China), rabbit monoclonal anti-phospho-Smad3 (Ser423/425) antibody (AF1759; Beyotime, China), rabbit monoclonal anti-TGF beta Receptor II antibody (Abcam; ab184948), and rabbit monoclonal anti-Smad4 antibody (AF1291; Beyotime, China). The secondary antibodies included FITC-labelled goat anti-rabbit IgG (H + L) (A0562; Beyotime, China), Alexa Fluor 488 (AF488)-labelled goat anti-mouse IgG (H + L) (A0428; Beyotime, China), HRP-labelled Goat Anti-Mouse IgG(H + L) (A0216; Beyotime, China), and HRP-labelled Goat Anti-Rabbit IgG(H + L) (A0208; Beyotime, China).

Preparation of CCD-18Co cell-derived conditioned medium (CM)

The CCD-18Co cells cultured for 4 generations were collected and washed three times with PBS to eliminate remnant FBS in the culture medium. Next, the cells were treated with serum-free medium for 48 h. The cell supernatants (called conditioned medium, CM) were collected and then were centrifuged at 1650 g for 3 min. A series of CCD-18Co cell-derived

CM with different percent values (from 12.5%, 25%, 50%, 75%, to 100%) was mixed with serum-free RPMI 1640 culture medium and pre-treated HCoEpiC.

3D culture model

To establish a 3D model, HCoEpiC were cultured on top of a thick layer of Cultrex® Basement Membrane Extract (BME). All the procedures were performed according to the specifications. Briefly, Cultrex® BME was thawed overnight at 4 °C and then was mixed by slowly pipetting the solution up and down, avoiding the introduction of air bubbles. Next, 200–300 μl per cm^2 of BME was pipetted into each well of a twelve-well culture plate, and the coated objects were incubated at 37 °C for 30 min to allow solidification. Subsequently, the objects were overlaid with 400 μl of complete medium containing 1×10^4 trypsinized cells and 3% Cultrex® BME. Finally, the cells were cultured for 7 days, and the medium was replaced with fresh medium every 2 or 3 days. Images of 3D morphology were acquired by phase contrast microscopy.

Co-culture model

A classical co-culture system is the Transwell model. Thus, CCD-18Co cells and HCoEpiC were co-cultured based on a Transwell system with a 3:1 cell number ratio to mimic the interactions between cells. In our co-culture system, 3×10^4 CCD-18Co cells were seeded into the 'bottom' chamber of a 24-mm Transwell plate and were incubated with 2 ml of DMEM (10% FBS). Next, 1×10^4 HCoEpiC were cultured with 1 ml of RPMI 1640 (10% FBS) onto the 'top' chamber of the Transwell plate. These cells were co-cultured for 24 h, 48 h, and 72 h (Fig. 1). Additionally, we created another co-culture model (named the direct co-culture model). Briefly, CCD-18Co cells (3×10^4) and HCoEpiC (1×10^4) were first cultured onto coverslips in a six-well culture plate. Because of their different media, HCoEpiC were domesticated with 50% DMEM and 50% RPMI 1640 to adapt to the subsequent co-culture condition. Next, the coverslips coated with the cells were placed into the same well of a six-well culture plate to culture for 24 h, 48 h, and 72 h (Fig. 1), and then 1 ml of DMEM (10% FBS) was added.

Treatment and induction of HCoEpiC by CM

Grouped HCoEpiC were seeded in a 6-well plate for 2D culture (Fig. 1). Twenty-four hours post seeding with 80%–90% cell confluence, the culture medium was replaced with or without the above different percent values of CCD-18Co cell-derived CM and was incubated for different time points (24 h, 48 h, and 72 h). The final volume in the 6-well plates was 2 ml. During incubation, these CM-treated HCoEpiC and control cells were photographed every 24 h using a phase-contrast microscope (Olympus). Additionally, three EMT markers (E-cadherin, vimentin, and α-SMA) were detected in these HCoEpiC. In the 3D-cultured HCoEpiC, the media of the formed multicellular spheroids were replaced with CM-containing media (serum-free), continuing the culture for 24 h, 48 h, 72 h (Fig. 1). Next, the morphological changes were observed using phase-contrast microscopy.

To inhibit the TGFβ/Smad pathway, HCoEpiC were pre-treated with LY 364947, a potent and selective ATP-competitive TGF-β receptor kinase I inhibitor; the treated concentrations were 0.18 nMol, 1.8 nMol, and 18 nMol for specified times (24 h and 48 h). Next, these cells were further induced by CCD-18Co-derived CM. In this situation, an optimal interventional effect was observed according to the phase-contrast microscope and aforementioned EMT

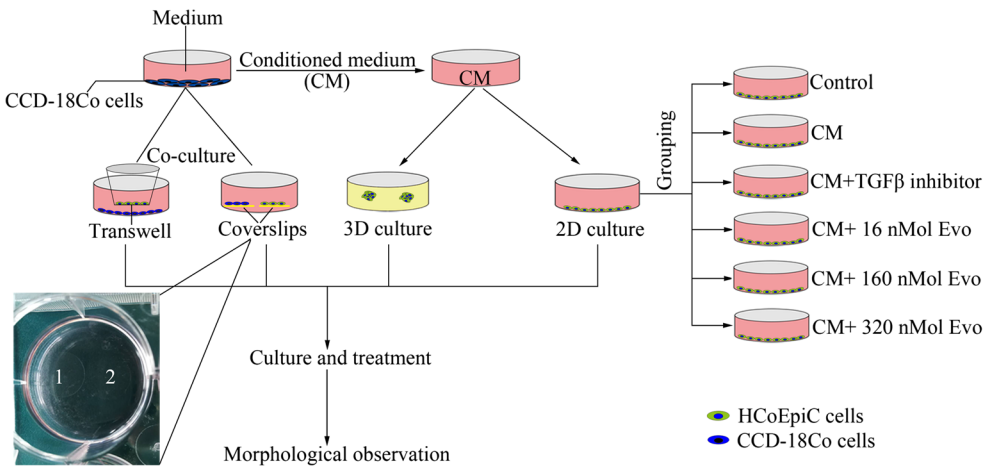

Fig. 1 Schematic diagram for our experimental design. CCD-18Co cells were cultured and extracted to acquire conditioned medium (CM). The Transwell system and direct co-culture model of CCD-18Co cells with the colon epithelial cell line HCoEpiC were established. HCoEpiC cultured in 2D and 3D models were treated with serum-free 25% CM. Additionally, HCoEpiC in the 2D model were divided into 6 groups. Morphological observation in the models was performed using a phase contrast microscope (Olympus). All the experiments were performed in triplicate, and the results were similar

markers. The cell sizes were measured using the image analysis software Image J (National Institutes of Health, America). Finally, the cells were harvested for subsequent experiments.

Cell migration detection by the wound healing assay

To perform the in vitro wound healing assay, cells were grown up to 90% confluence in 35-mm dishes. First, a wound of the cell layer was generated using a sterile 200-μl pipette tip, followed by incubation of serum-free culture medium (with or without CM) for 24 h. Observation of the wound was carried out at 0 h, 6 h, 12 h, 18 h, and 24 h, and the corresponding images were also collected using a phase contrast microscope. Next, the degree of healing was measured and quantified according to the areas of the wound by image analysis software Image J (National Institutes of Health, America).

Immunofluorescence (IF) staining

HCoEpiC were plated on 15-mm coverslips pre-placed into 6-well plates, followed by incubation for 24 h. The media were replaced with fresh serum-free media containing 25% CCD-18Co CM, and culture was continued for another 24 h. The cells undergoing EMT were then treated with evodiamine at different concentrations, 18 nMol of LY 364947, and 0.1% DMSO for another 48 h. All the cells were washed three times with PBS (pH 7.4), fixed with 4% paraformaldehyde for 20 min, and permeabilized with 0.5% Triton X-100 solution for 30 min (permeabilization of E-cadherin was needless). Next, these cells were incubated for 30 min in blocking solution (PBS supplemented with 10% sheep serum). After the blocking solution was removed, the coverslips were incubated with anti-E-cadherin (1:200), −vimentin (1:300), and -α-SMA (1:300) primary antibodies at 4 °C overnight. They were then washed with PBST (PBS supplemented with 0.05% Tween-20) and incubated with goat anti-mouse AlexaFluor-488 antibodies (E-cadherin) and goat anti-rabbit FITC antibodies (vimentin and α-SMA) for 2 h at 37 °C. The cell nuclei were counterstained with 4′,6-diamidino-2-phenylindole (DAPI) (C1005; Beyotime, China) for 3 min at room temperature. The coverslips were again washed three times with PBST and were covered with antifade mounting reagent. Observation was performed under a fluorescence microscope (Olympus) equipped with a 960S-Fluor oil immersion lens. Additionally, the mean fluorescence intensity of each image was calculated using Image-Pro®Plusv6.0 (Media Cybernetics, USA). For representation, the images were deconvoluted with the deconvolve three-dimensional (3D) plugin 61 of Image-Pro®Plusv6.0. The deconvoluted image was pseudo-coloured, and a surface plot was generated using IPP 6.0.

To quantify the changes in fluorescence, the images were processed using the Image Pro plus software, Image-Pro®Plusv6.0. A region of interest (ROI) was drawn around each cell, and the mean density = (IOD SUM)/(area SUM). Briefly, the images were converted to those with a grey scale of 8, and contrast was inverted. The raw intensities were normalized to the mean intensity of the integral optical density (IOD) for each cell. The IOD and area of the ROI in each cell were measured. Next, IOD SUM and area SUM were calculated using view statistics in this software.

Western blotting analysis

Protein extracts were prepared and run as previously described [10]. Briefly, 10 μg of each protein sample was separated by 10% SDS-PAGE gel and electrotransferred onto a PVDF membrane at 120 V for 1 h. Subsequently, the membranes were blocked in Tris-buffered saline Tween (TBST) buffer (20 mM Tris-HCl, pH 7.6, 150 mM NaCl, 0.1% Tween-20) with 10% non-fat milk at 25 °C for 2 h. Next, the membranes were incubated with the following diluted specific primary antibodies at 4 °C overnight: E-cadherin (1:500), vimentin (1:1000), α-SMA (1:1000), ZEB1 (1:1000), Snail (1:1000), TβRII (1:1000), Smad2 (1:500), Smad3 (1:500), ph-Smad2 (1:500), ph-Smad3 (1:500), Smad4 (1:500), and β-actin (1:1000). These blotted proteins were subsequently incubated with the corresponding horseradish peroxidase (HRP)-conjugated secondary antibody (1:1000) for 2 h at room temperature (25 °C). Molecular Imager ® Chemi Doc™ XR+ system with Image Lab TM Software (Bio-Rad) was used to acquire all protein bands and intensities.

Statistical analysis

All the data were analysed according using the statistical software SPSS 20.0, and a two-tailed test was used in this study. The data were presented as the mean (M) ± standard deviation (SD). Differences were considered to be significant if the P value was less than 0.05 ($^*P < 0.05$). All the data were representative of at least three different experiments.

Results

EMT-like phenotype transition in the colon epithelial cell line HCoEpiC

Although fibroblasts resident in the tumour microenvironment (TME) have been termed various names including peritumoural (myo-)fibroblasts, cancer-associated fibroblasts (CAFs) or tumour-associated fibroblasts (TAFs), and present some difference with normal fibroblasts [11, 12], them express common biomarkers, such as α-SMA, fibroblast surface protein (FSP1) and fibroblast-activated protein (FAP) [11, 12].

Increasingly evidence has shown involvement of TAFs in tumour initiation and development. These processes are

largely driven by their secretion of multiple cytokines and growth factors which have influence on proliferation, adhesion and migration of tumour cells [13, 14]. Perhaps the promotion of tumour cell invasion and migration is the best-understood function for TAFs. One of the underlying mechanisms is the induction of the epithelial-to-mesenchymal transition (EMT). EMT is initiated by secreted matrix metalloproteases or cytokines such as transforming growth factor-β (TGF-β).

TAFs also affect other stroma cells in TME [15], including epithelial cells. To verify this notion, we first used the conditioned medium (CM) from CCD18-Co cells, a myofibroblast cell line [16]. CCD18-Co myofibroblasts play an important role in the remodelling of the surrounding matrix [17], similar to the function of TAFs in microenvironment remodelling [18]. Thus, in our experiment, we selected the CCD18-Co cell line as the TAF model to evaluate the stromal-epithelial interactions.

We observed, for the first time, that 25% CM with serum-free RPMI 1640 induced spindle-like morphological changes in 2D-cultured HCoEpiC after a 24-h treatment compared with the control (RPMI 1640 with CM-free), as shown in Fig. 2. To better mimic the communication between the two cells types, we found a similar phenomenon in the Transwell model (Fig. 3). Additionally, based on co-culture, we innovatively used a direct co-culture system in which CCD-18Co cells and HCoEpiC grew in the same environment for 24 h. Exciting results also revealed the spindle-shape morphological change in the treated HCoEpiC, as shown in Fig. 3. Interestingly, under 3D culture, after 5 days with 25% serum-free CM stimulation, some dispersive cells appeared in the periphery of HCoEpiC organoids (Fig. 3) compared with those in the blank control (serum-free without CM), suggesting the occurrence of cell migration. Enhanced migration is a behaviour of the strengthened motility of cells undergoing EMT [19]. In the presence of CCD-18Co CM, the migration of the cells was obviously promoted (Fig. 4), in contrast to the cells without CM treatment (Fig. 4). These observations demonstrated that EMT-like HCoEpiC are induced and exhibit enhanced migration abilities under CCD-18Co CM stimulation.

Additionally, fluorescence staining revealed that the expression of epithelial marker E-cadherin was down-regulated, while that of the mesenchymal markers α-SMA and vimentin was high-expressed, compared with the control (Fig. 5). The relative transcription factors ZEB1 and Snail responsible for EMT induction were also up-regulated in their protein expression (Fig. 6).

Taken together, these observations indicate that in vitro EMT-like changes of HCoEpiC can be induced by CCD-18Co cells and may be associated with some active factors

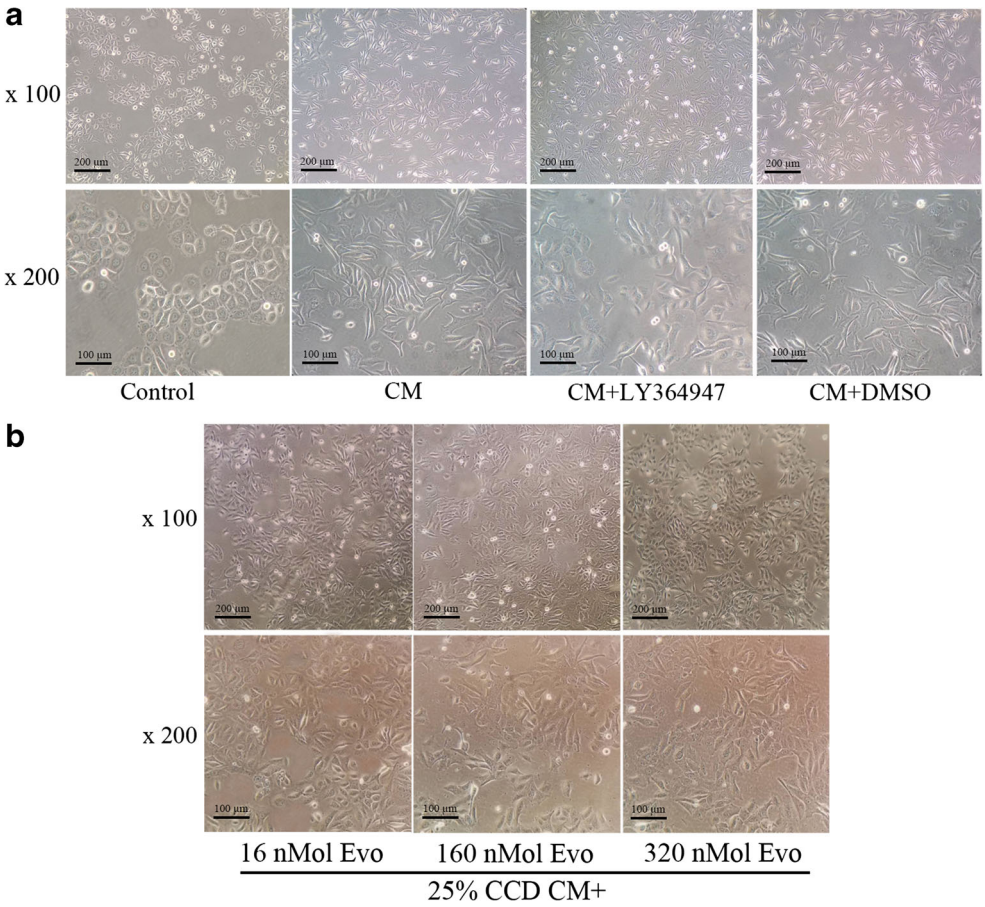

Fig. 2 HCoEpiC were treated with 25% CCD-18Co-derived CM, and the EMT-like HCoEpiC were treated with evodiamine at different doses. **a** In the CM group, HCoEpiC were treated with 25% CM for 24 h. In the CM + LY364947 group, the cells were co-treated with 25% CM and 18 nMol of LY364947 for 24 h. **b** After HCoEpiC were pre-treated with 25% CM for 24 h, they were treated with evodiamine at 16 nMol, 160 nMol, or 320 nMol for another 24 h. All morphological observations were acquired using a phase contrast microscope (Olympus). Bars = 200 μm and 100 μm for × 100 and × 200 magnifications, respectively

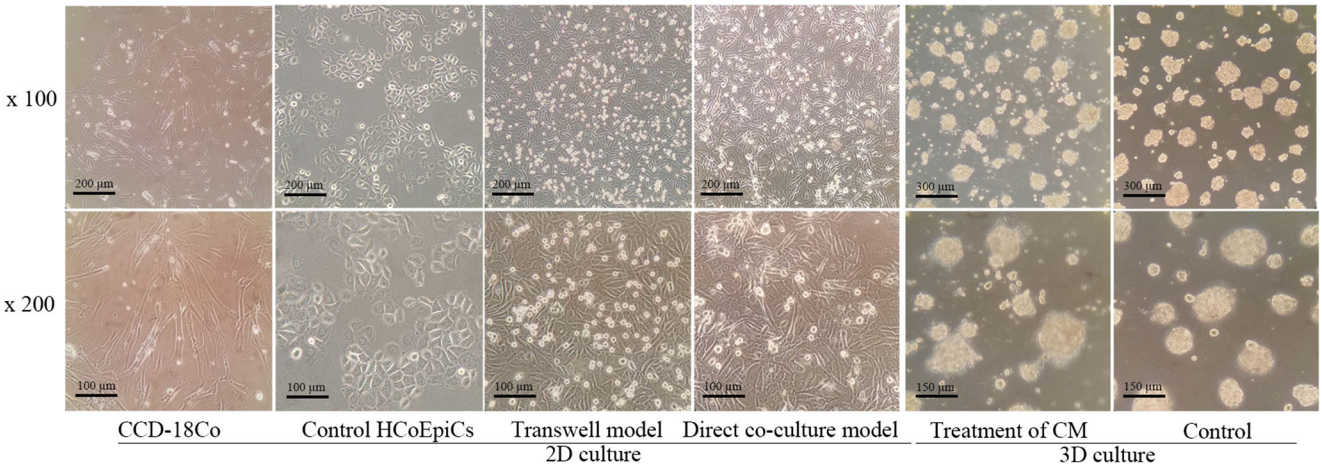

Fig. 3 Induction of CCD-18Co in 2D- and 3D-cultured HCoEpiC. In the 2D-cultured cells, two models, Transwell and direct co-culture, were used. The morphological features between CCD-18Co and HCoEpiC were different. CCD-18Co cells presented were spindle shaped, with a wide intercellular space and prolonged cell length, while HCoEpiC were characterized by a "paving stone" and polygonal shape with a tight intercellular space. CCD-18Co cells and HCoEpiC in the two models were co-cultured for 24 h. Bars in the 2D model = 200 μm and 100 μm for × 100 and × 200 magnifications, respectively. In the 3D-cultured model, when the multicellular spheroids were formed, the cells were treated with 25% CCD-18Co CM for 5 days. The control group comprised HCoEpiC without CCD-18Co treatment. Bars in the 3D model = 300 μm and 150 μm for × 100 and × 200 magnifications, respectively

secreted by the latter. To further extend and explore these observations, a TGF-β receptor kinase I inhibitor LY364947 was used. We found that the EMT-like changes of HCoEpiC induced by CM were inhibited by 18 nMol LY364947 (Fig. 2). Additionally, the expression of E-cadherin was increased and that α-SMA and vimentin was decreased (Fig. 5). The levels of ZEB1 and Snail were also down-regulated by the intervention of LY364947 (Fig. 6).

Dysregulated TGF-β/Smad signalling during the CCD-18Co CM-induced EMT in the HCoEpiC

The above results indicated that in vitro EMT in HCoEpiC can be induced by CCD-18Co cells, and this induction may be driven by TGF-β. To further explore and confirm the theory, we detected TGF-β/Smad signalling using western blotting.

The binding of TGF-β to TGF-β receptors (TβRI and TβRII) promotes Smad2/3/4 complex formation and translocation to the nucleus (Smad pathway), leading to transcriptional regulation of multiple target genes [20]. Thus, this classical Smad pathway plays an important role in TGF-β-induced tumour suppressor functions in normal epithelium and in the early stage of tumour progression [21]. Notably, among these targets mediated by Smads, some genes are related to EMT [22]. As shown in Fig. 6, TβRII expression was increased during the EMT of HCoEpiC. Simultaneously, increased expression levels of classical Smads, including Smad2 and Smad3, were observed in the EMT-like HCoEpiC. Additionally, as a common molecular partner of receptor-regulated Smads (RSmads), Smad4 in the nucleus and RSmads (Smad2 and Smad3) form a complex associated with additional DNA-binding cofactors, and then binding with high affinity and selectivity to specific target genes are achieved [23]. In this scenario, TGF-β stimulates the occurrence of EMT through Smad-dependent transcriptional events. As shown in our study, with CM treatment, high-expressed Smad4 appeared in HCoEpiC undergoing EMT. Surprisingly, both pSmad2 and pSmad3 expression levels were down-regulated (Fig. 6). Additionally, CCD-18Co reduced the ratios of pSmad2/Smad2 and pSmad3/Smad3 (Fig. 6). With the addition of LY364947, the above phenomena were inverted (Fig. 6).

These observations suggest that the dysregulation of TGF-β/Smad signalling is activated in HCoEpiC undergoing EMT induced by CM from CCD-18Co cells, and TGF-β may be involved in the communication between epithelial cells and TAFs.

Reversion of EMT and repression of migration by evodiamine

As a natural product, evodiamine (Evo) exerts multiple pharmacological anti-cancer activities, including cytotoxicity [8], inhibition of cell migration and invasion. These activities are related to Raf/MEK/ERK signalling [9] or repression of MMP-2 expression [24]. Additionally, a study by Wei has shown that evodiamine inhibits TGF-beta1-induced EMT in NRK52E cells via the Smad and PPAR-gamma pathway [22]. However, whether Evo has the same inhibitory effects on TAF-induced EMT in colon epithelial cells remains unknown.

As expected, 160 nMol and 320 nMol Evo significantly reverted the EMT transition of HCoEpiC (Fig. 2). Similarly, we found the inhibitory effect of Evo on the migration of HCoEpiC undergoing EMT, especially at 160 nMol and 320 nMol Evo ($P < 0.05$) (Fig. 4), but its effect was not obvious

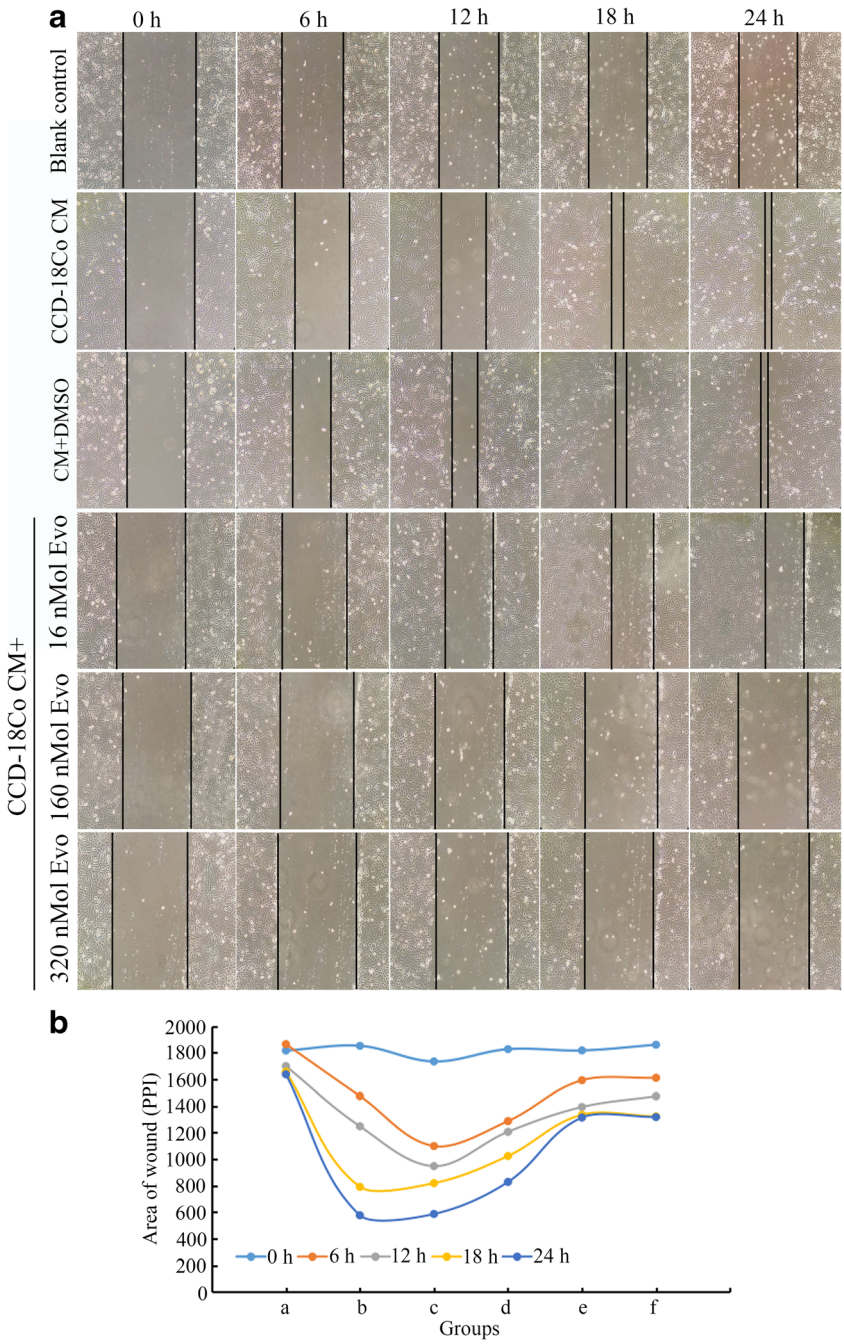

Fig. 4 Analysis of HCoEpiC motility by the wound-healing assay. **a** Cultured HCoEpiC were analysed by phase contrast microscopy (10 × 10). **b** Analysis of the wound area by Image J, with the area of the wound presented as pixels per inch (PPI). **a**: Blank control, **b**: CCD-18Co CM, **c**: CCD-18Co CM + LY364947, **d**: CCD-18Co CM + 16 nMol Evo, **e**: CCD-18Co CM + 160 nMol Evo, **f**: CCD-18Co CM + 320 nMol Evo

at 16 nMol. Additionally, its anti-migration effect seems not to be associated with the doses of Evo due to no statistical significance between 160 nMol and 320 nMol. The observations revealed that the repressive effect of Evo on migration needs to reach a certain dose. As shown in Fig. 5, Evo promoted de novo expression of E-cadherin and down-regulation of α-SAM and vimentin ($P < 0.05$) in a dose-dependent manner compared with the CCD-18Co CM group. Although its influence on α-SAM is non-significant at the protein level (Fig. 5e-f), Evo indeed exerted the activities of anti-EMT and anti-migration.

Regulation of pSmad2/3 in the TGF-β pathway by evodiamine

The aforementioned results have revealed the anti-EMT and anti-migration effects of Evo. Thus, we determined whether these effects occurred through the regulation of TGF-β/Smad signalling. We found that Evo remarkably reduced the expression levels of ZEB1 and Snail ($P < 0.05$, Fig. 6), especially at 160 nMol and 320 nMol. The results demonstrated that Evo can revert EMT, which is consistent with the results of other studies [22, 25], although its effect on ZEB1 was not obvious at 320 nMol compared with the CCD-18Co CM group.

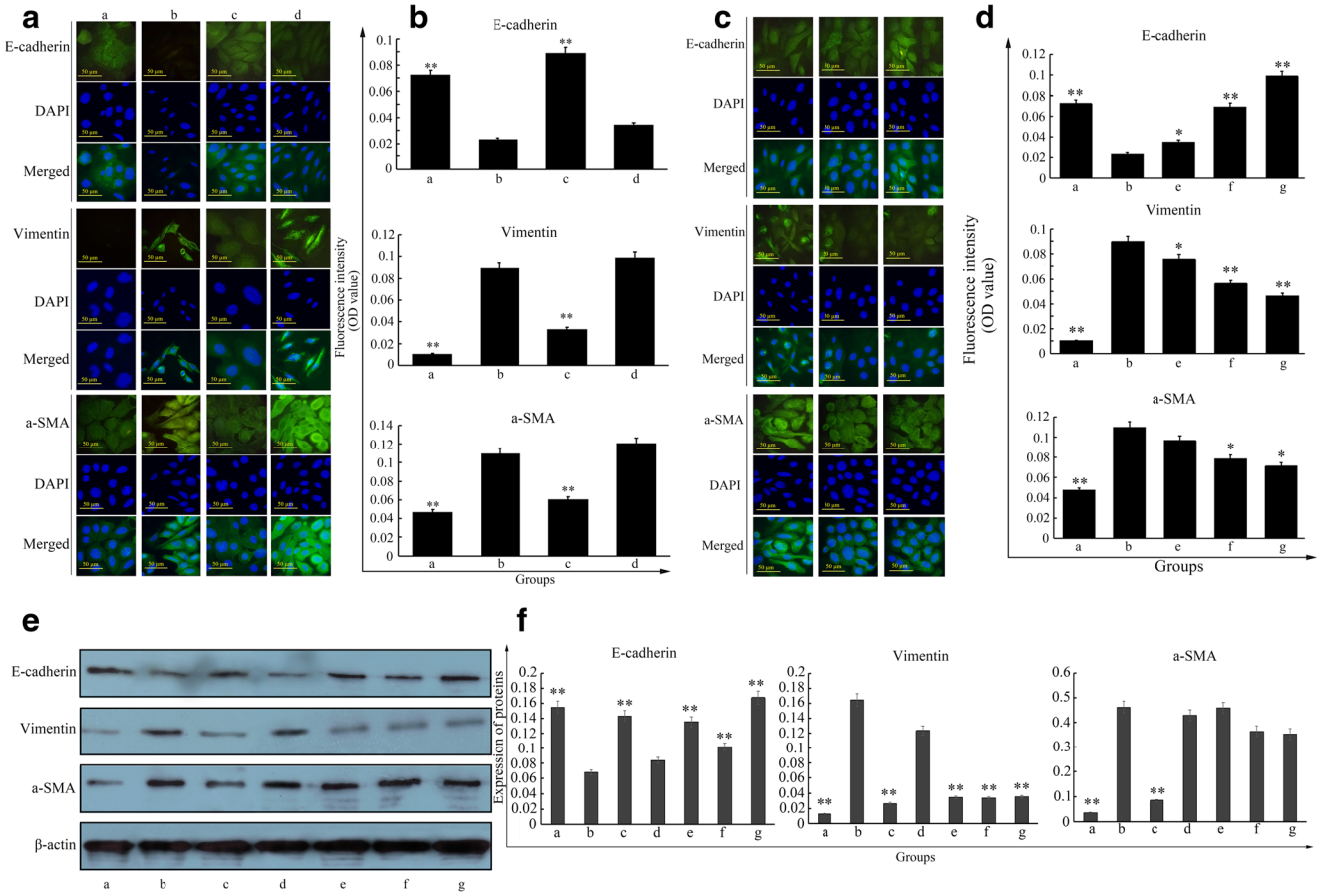

Fig. 5 Immunofluorescence to detect EMT markers using a fluorescence microscope (Olympus) equipped with a 960S-Fluor oil immersion lens (10 × 100) and detection by WB. (**a** and **c**) Fluorescence of target proteins. (**b** and **d**) Detection of fluorescence intensity. (**e** and **f**) Detection of Western blotting of EMT markers. Green fluorescence of E-cadherin was detected by AF488 (Alexa Flour488) staining, while green fluorescence of vimentin and α-SMA was detected by fluorescein isothiocyanate (FITC) staining. Cell nucleus counterstaining was performed using DAPI. **a**: Control, **b**: CCD-18Co CM, **c**: CCD-18Co CM + LY364947, **d**: CCD-18Co CM + DMSO, **e**: CCD-18Co CM + 16 nMol Evo, **f**: CCD-18Co CM + 160 nMol Evo, **g**: CCD-18Co CM + 320 nMol Evo. The error bar represents the SD ($n = 3$). $^{*}P < 0.05$ and $^{**}P < 0.01$ versus the CCD-18Co CM group. Bar = 50 μm

Additionally, LY364947 reduced the expression levels of TβRII, Smad2 and Smad3, but these expression levels were not influenced by Evo (Fig. 6). By contrast, Evo increased the levels of pSmad2 and pSmad3 expression ($P < 0.05$, Fig. 6), a finding that is consistent with the effect of LY364947. We observed that the effect of Evo may be related to the increased ratio between phosphorylated Smad2/3 (pSmad2/3) and unphosphorylated Smad2/3 (Smad2/3). As shown in Fig. 6c, Evo significantly up-regulated the ratios of p-Smad2/Smad and p-Smad3/Smad3.

As a TGF-β signal mediator, Smad4 is required for EMT, and its frequent inactivation or decreased expression is often observed in gastrointestinal cancers [26]. EMT induced by TGF-β is generally considered to be a pro-tumourigenic event [26], suggesting the tumour-promoting behaviour of Smad4. CCD-18Co dramatically promoted the expression of Smad4 in HCoEpiC, consistent with the pro-EMT ability of Smad4. Hence, inhibition of Smad4 becomes a good strategy. In this study, we found that 16 nMol of and 160 nMol of Evo down-regulated the level of Smad4, but 320 nMol of Evo significantly promoted its expression ($P < 0.05$, Fig. 6), suggesting that the expression of Smad4 may be drug concentration relevant.

Together, these observations demonstrated that evodiamine reverses the EMT of colon epithelial cells induced by TAFs in relation to the mediation of pSmad2/3 expression in the TGF-β pathway.

Discussion

Stromal cells are the primary components in the tumour microenvironment (TME). These cells contribute to carcinogenic initiation and development [27]. The pro-tumoural fibroblasts (also named as myofibroblasts) possess abundant and heterogeneous origination [28]. Resident fibroblasts from colon tissues are the most possible cellular source of TAFs in colorectal cancer [6]. These myofibroblasts synthesize various types of collagens and extracellular matrix (ECM) proteins to provide a scaffold for

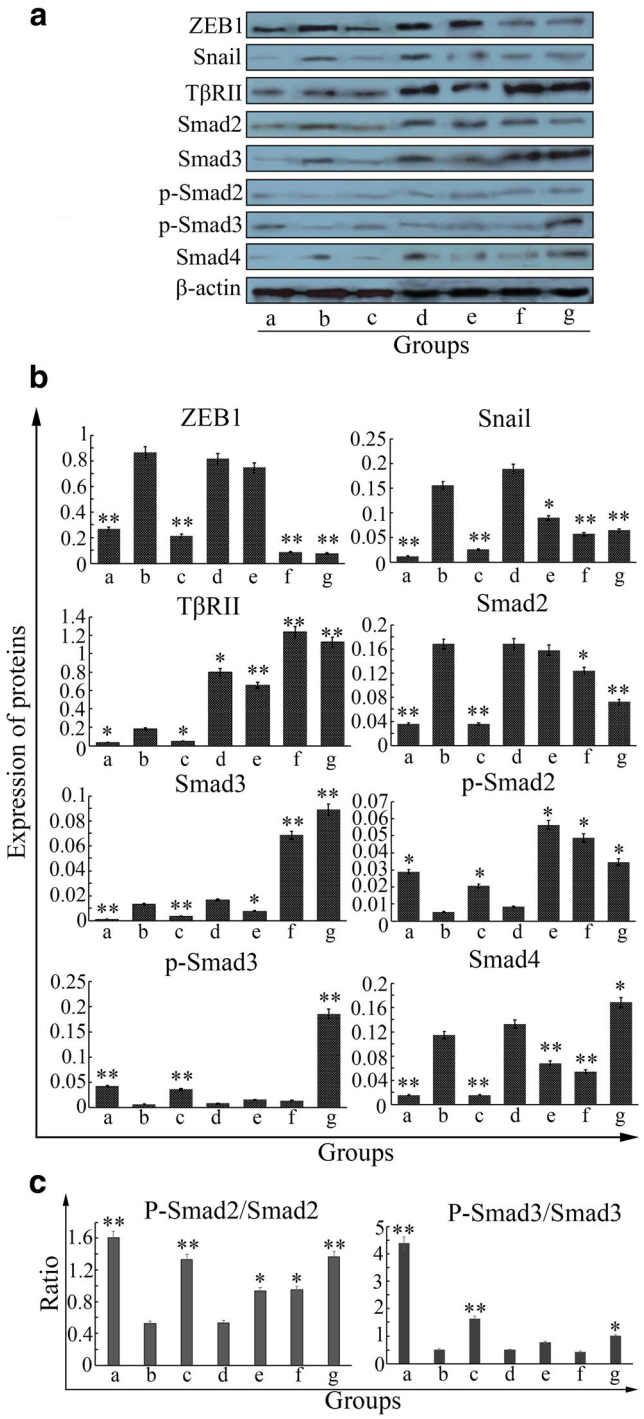

Fig. 6 Detection of the expression of EMT transcription factors, TGF-β receptors, and Smads by western blotting. **a** Protein bands of western blot analysis in the cells treated with different conditions. **b** Analysis of the expression of the protein bands. **c** Ratio between phosphorylated Smad2/3 and unphosphorylated Smad2/3. **a**: Control, **b**: CCD-18Co CM, **c**: CCD-18Co CM + LY364947, **d**: CCD-18Co CM + DMSO, **e**: CCD-18Co CM + 16 nMol Evo, **f**: CCD-18Co CM + 160 nMol Evo, **g**: CCD-18Co CM + 320 nMol Evo. The error bar represents the SD (n = 3). $^{*}P < 0.05$ and $^{**}P < 0.01$ versus the CCD-18Co CM group

tumour growth and development [29]. Additionally, they secrete numerous growth factors and cytokines enriched in the TME to reinforce the communication between cancer cells and stromal cells or between stromal cells [30].

Similar to TAFs, human colon CCD-18Co myofibroblasts can remodel the ECM [17, 31]. Therefore, we used CCD-18Co as our TAF model to explore the interaction between TAFs and epithelial cells. Our results have shown that conditioned medium (CM) or the co-culture of CCD-18Co induced in vitro epithelial-mesenchymal transition (EMT)-like changes in 2D- or 3D-cultured colon epithelial HCoEpiC. These EMT-like HCoEpiC present the reduction of E-cadherin and enhancement of vimentin and α-SMA, with high expression of Snail and ZEB1. Interestingly, these phenomena can be abolished by the TGF-β receptor kinase I inhibitor LY364947, indicating that CCD-18Co cells produce a certain amount of TGF-β. The CCD-18Co-derived TGF-β enhances the communication between CCD-18Co and epithelial cells through the induction of EMT. Novel studies have revealed that much of the TGF-β produced by TAFs can strengthen the stromal reaction and induce the transdifferentiation of epithelial cells, and the TGF-β signalling pathway is the primary inducer of EMT in various tumour types [15, 32].

In this context, the CCD-18Co-derived TGF-β signal functions through type I and II TGF-β receptors (TβRI and TβRII). TβRII binding to TGF-β ligand recruits and phosphorylates TβRI. This heterodimer complex activates and phosphorylates downstream mediators Smad2 and Smad3 to induce the combination with Smad4 and its entrance into the nucleus. Existing substantial evidence has demonstrated that the classical TGF-β/Smad signalling pathway is closely associated with cell proliferation, differentiation and migration [33]. However, in our study, we determined whether the TGF-β signalling is activated in the pro-EMT process. Subsequent results have revealed that CCD-18Co CM increases the expression levels of TβRII, Smad2, Smad3 and Smad4, suggesting that TGF-β/Smad signalling is activated in EMT. Recent studies have reported that the over-activation of TGF-β-Smad2 signalling promotes the establishment of EMT by maintaining the epigenetic silencing of key epithelial marker genes, such as E-cadherin [34]. Although the functions of Smad4 in colorectal cancer are not entirely clear, the positive correlation of Smad4 with EMT transcription factors Snail-1, Slug and Twist-1 expression was found in colon tumour specimens [35]. Because Smad4 is an essential protein of the TGF-β pathway, we consider that up-regulated Smad3 and Smad4 contributes to the EMT process induced by CCD-18Co.

In addition to the changes of Smad2/3/4, after treatment with CCD-18Co-derived CM, the expression levels of pSmad2 and pSmad3 and the ratios of pSmad2/Smad2 and pSmad3/Smad3 were reduced. These results suggest that the reduction of pSmad2/3 may be the dominant factor resulting in EMT. In a study by Dong [36], TGF-β1 induced the up-regulation of pSmad3 during EMT. However, staining for

pSmad2/3 was dramatically reduced in the epithelial cells of colorectal cancer, in contrast to adjacent stromal cells or the epithelial compartment of pre-malignant tissue [15]. These data suggest the mysterious roles of pSmad2 or pSmad3 during the process of EMT and tumourigenesis, and further exploration will be needed to confirm this impression.

Evodiamine (Evo) has potent anti-cancer effects, including the arrest of cell growth and induction of apoptosis [8, 9, 24, 37]. Some studies have found that Evo represses TGF-β1-induced EMT in rat renal proximal tubular epithelial cells [22]. However, the effect of Evo on EMT induced by TAFs and the underlying mechanisms remain vague. In the present study, we have found that Evo exerts potential anti-EMT and anti-migration activities, which are consistent with the previous results. The results indicated that Evo promotes the differentiation of mesenchymal cells, which has been confirmed by another study in which Evo promotes the differentiation in C2C12 muscle cells [38].

TGF-β signalling is a master mediator of EMT, and Smads are crucial components in this pathway. Orchestrating the TGF-β/Smad signalling pathway is a promising strategy. Our results have demonstrated that CCD-18Co-stimulated HCoEpiC EMT and migration were significantly suppressed by 160 nMol and 320 nMol of Evo ($P < 0.05$). Further detection found that Evo (160 nMol and 320 nMol) significantly down-regulated the levels of Snail and ZEB1, suggesting that Evo plays an anti-EMT role in relation to the regulation of ZEB1 and Snail. After intervention with a TGF-β inhibitor LY364947, TβRII, Smad2, Smad3 and Smad4 expressions were down-regulated, accompanied with the up-regulation of pSmad2 and pSmad3 (Fig. 6). However, after treatment with Evo, the expression levels of TβRII, Smad2 and Smad3 presented an increasing trend. Additionally, although 320 nMol of Evo increased the expression levels of Smad4, 16 nMol and 160 nMol of Evo reduced its expression, suggesting that the effect of Evo on Smad4 is likely associated with the drug concentration.

Evo dramatically increased the expression of pSmad2/3 and Smad2/3. Therefore, we deemed that the anti-EMT function of Evo is mainly related to the up-regulation of pSmad2/3 or Smad2/3 expression. However, LY364947 and Evo obviously increased the ratios of pSmad2/Smad2 and p-Smad3/Smad3, indicating that Evo functions through regulating the ratios of p-Smad2/Smad2 and p-Smad3/Smad3.

In summary, TGF-β may be an effector for CCD-18Co cells in communication with colon epithelial HCoEpiC, and Evo reverts the EMT-like changes of HCoEpiC induced by CCD-18Co and represses migration through mediating the expression levels of pSmad2 and pSmad3 or the ratios of pSmad2/Smad2 and p-Smad3/Smad3.

Acknowledgements Bo Liu, PhD, and Cun-jia Zhang, PhD, provided medical writing support.

Funding The work was supported by the Natural Science Foundation of Guangdong Province (2018A030310060) and PhD Initial Foundation of Hospital (20170916).

Compliance with ethical standards

Conflict of interest Wan bin Yang declares that he has no conflict of interest. Xiu li Gong declares that she has no conflict of interest. Xiu lian Wang declares that she has no conflict of interest. Chao Huang declares that he has no conflict of interest.

Ethical approval This article does not contain any studies with human participants or animals performed by any of the authors.

Informed consent For this type of study, formal consent is not required.

References

1. Servais C, Erez N (2013) From sentinel cells to inflammatory culprits: cancer-associated fibroblasts in tumour-related inflammation. J Pathol 229:198–207
2. Glentis A, Oertle P, Mariani P, Chikina A, El Marjou F, Attieh Y et al (2017) Cancer-associated fibroblasts induce metalloprotease-independent cancer cell invasion of the basement membrane. Nat Commun 8(1):924
3. Kojima Y, Acar A, Eaton EN, Mellody KT, Scheel C, Ben-Porath I, onder TT, Wang ZC, Richardson AL, Weinberg RA, Orimo A (2010) Autocrine TGF-beta and stromal cell-derived factor-1 (SDF-1) signaling drives the evolution of tumor-promoting mammary stromal myofibroblasts. Proc Natl Acad Sci U S A 107: 20009–20014
4. Achyut BR, Yang L (2011) Transforming growth factor-β in the gastrointestinal and hepatic tumor microenvironment. Gastroenterology 141(4):1167–1178
5. Neuzillet C, Tijeras-Raballand A, Cohen R, Cros J, Faivre S, Raymond E, de Gramont A (2015) Targeting the TGFβ pathway for cancer therapy. Pharmacol Ther 147:22–31
6. Mukaida N, Sasaki S (2016) Fibroblasts, an inconspicuous but essential player in colon cancer development and progression. World J Gastroenterol 22(23):5301–5316
7. Guarino M, Tosoni A, Nebuloni M (2009) Direct contribution of epithelium to organ fibrosis: epithelial-mesenchymal transition. Hum Pathol 40:1365–1376
8. Yu HI, Chou HC, Su YC, Lin LH, Lu CH, Chuang HH, Tsai YT, Liao EC, Wei YS, Yang YT, Lee YR, Chan HL (2018) Proteomic analysis of evodiamine-induced cytotoxicity in thyroid cancer cells. J Pharm Biomed Anal 160:344–350
9. Zhou Y, Hu J (2018) Evodiamine induces apoptosis, G2/M cell cycle arrest, and inhibition of cell migration and invasion in human osteosarcoma cells via Raf/MEK/ERK Signalling pathway. Med Sci Monit 24:5874–5880
10. Huang C, Wen B (2016) Phenotype transformation of immortalized NCM460 colon epithelial cell line by TGF-β1 is associated with chromosome instability. Mol Biol Rep 43:1069–1078
11. Bauer M, Su G, Casper C, He R, Rehrauer W, Friedl A (2010) Heterogeneity of gene expression in stromal fibroblasts of human breast carcinomas and normal breast. Oncogene 29(12):1732–1740
12. Navab R, Strumpf D, Bandarchi B, Zhu CQ, Pintilie M, Ramnarine VR, Ibrahimov E, Radulovich N, Leung L, Barczyk M, Panchal D,

To C, Yun JJ, der S, Shepherd FA, Jurisica I, Tsao MS (2011) Prognostic gene-expression signature of carcinoma-associated fibroblasts in non-small cell lung cancer. Proc Natl Acad Sci U S A 108(17):7160–7165
13. De Wever O, Demetter P, Mareel M, Bracke M (2008) Stromal myofibroblasts are drivers of invasive cancer growth. Int J Cancer 123(10):2229–2238
14. Calon A, Tauriello DV, Batlle E (2014) TGF-beta in CAF-mediated tumor growth and metastasis. Semin Cancer Biol 25:15–22
15. Lakins MA, Ghorani E, Munir H, Martins CP, Shields JD (2018) Cancer-associated fibroblasts induce antigen-specific deletion of CD8 + T cells to protect tumour cells. Nat Commun 9(1):948
16. Giménez-Bastida JA, Surma M, Zieliński H (2015) In vitro evaluation of the cytotoxicity and modulation of mechanisms associated with inflammation induced by perfluorooctanesulfonate and perfluorooctanoic acid in human colon myofibroblasts CCD-18Co. Toxicol in Vitro 29(7):1683–1691
17. Pereira C, Araújo F, Barrias CC, Granja PL, Sarmento B (2015) Dissecting stromal-epithelial interactions in a 3D in vitro cellularized intestinal model for permeability studies. Biomaterials 56:36–45
18. Chen Q, Liu G, Liu S, Su H, Wang Y, Li J, Luo C (2018) Remodeling the tumor microenvironment with emerging Nanotherapeutics. Trends Pharmacol Sci 39(1):59–74
19. Papageorgis P (2015) TGFβ signaling in tumor initiation, epithelial-to-mesenchymal transition, and metastasis. J Oncol 2015:587193
20. Fearon ER (2011) Molecular genetics of colorectal cancer. Annu Rev Pathol 6:479–507
21. Lyu G, Guan Y, Zhang C, Zong L, Sun L, Huang X, Huang L, Zhang L, Tian XL, Zhou Z, Tao W (2018) TGF-β signaling alters H4K20me3 status via miR-29 and contributes to cellular senescence and cardiac aging. Nat Commun 9(1):2560
22. Wei J, Li Z, Yuan F (2014) Evodiamine might inhibit TGF-beta1-induced epithelial-mesenchymal transition in NRK52E cells via Smad and PPAR-gamma pathway. Cell Biol Int 38(7):875–880
23. Massagué J (2008) TGFbeta in Cancer. Cell 134(2):215–230
24. Peng X, Zhang Q, Zeng Y, Li J, Wang L, Ai P (2015) Evodiamine inhibits the migration and invasion of nasopharyngeal carcinoma cells in vitro via repressing MMP-2 expression. Cancer Chemother Pharmacol 76(6):1173–1184
25. Wen Z, Feng S, Wei L, Wang Z, Hong D, Wang Q (2015) Evodiamine, a novel inhibitor of the Wnt pathway, inhibits the self-renewal of gastric cancer stem cells. Int J Mol Med 36(6):1657–1663
26. David CJ, Huang YH, Chen M, Su J, Zou Y, Bardeesy N, Iacobuzio-Donahue CA, Massagué J (2016) TGF-β tumor suppression through a lethal EMT. Cell 164(5):1015–1030
27. Vera-Ramirez L, Sanchez-Rovira P, Ramirez-Tortosa CL, Quiles JL, Ramirez-Tortosa MC, Alvarez JC, Fernandez-Navarro M, Lorente JA (2010) Gene-expression profiles, tumor microenvironment, and cancer stem cells in breast cancer: latest advances towards an integrated approach. Cancer Treat Rev 36:477–484
28. Bussard KM, Mutkus L, Stumpf K, Gomez-Manzano C, Marini FC (2016) Tumor-associated stromal cells as key contributors to the tumor microenvironment. Breast Cancer Res 18(1):84
29. Klingberg F, Hinz B, White ES (2013) The myofibroblast matrix: implications for tissue repair and fibrosis. J Pathol 229:298–309
30. Werner S, Grose R (2003) Regulation of wound healing by growth factors and cytokines. Physiol Rev 83:835–870
31. Giménez-Bastida JA, Laparra-Llopis JM, Baczek N, Zielinski H (2018) Buckwheat and buckwheat enriched products exert an anti-inflammatory effect on the myofibroblasts of colon CCD-18Co. Food Funct 9(6):3387–3397
32. McDonald LT, LaRue AC (2012) Hematopoietic stem cell derived carcinoma-associated fibroblasts: a novel origin. Int J Clin Exp Pathol 5(9):863–873
33. Ji Q, Liu X, Han Z, Zhou L, Sui H, Yan L, Jiang H, Ren J, Cai J, Li Q (2015) Resveratrol suppresses epithelial-to-mesenchymal transition in colorectal cancer through TGF-β1/Smads signaling pathway mediated snail/E-cadherin expression. BMC Cancer 15:97
34. Dong F, Liu T, Jin H, Wang W (2018) Chimaphilin inhibits human osteosarcoma cell invasion and metastasis through suppressing the TGF-β1-induced epithelial-to-mesenchymal transition markers via PI-3K/Akt, ERK1/2, and Smad signaling pathways. Can J Physiol Pharmacol 96(1):1–7
35. Ioannou M, Kouvaras E, Papamichali R, Samara M, Chiotoglou I, Koukoulis G (2018) Smad4 and epithelial-mesenchymal transition proteins in colorectal carcinoma: an immunohistochemical study. J Mol Histol 49(3):235–244
36. Dong Z, Tai W, Lei W, Wang Y, Li Z, Zhang T (2016) IL-27 inhibits the TGF-β1-induced epithelial-mesenchymal transition in alveolar epithelial cells. BMC Cell Biol 17:7
37. Su T, Yang X, Deng JH, Huang QJ, Huang SC, Zhang YM, Zheng HM, Wang Y, Lu LL, Liu ZQ (2018) Evodiamine, a novel NOTCH3 methylation stimulator, significantly suppresses lung carcinogenesis in vitro and in vivo. Front Pharmacol 9:434. https://doi.org/10.3389/fphar.2018.00434
38. Yao X, Yu T, Zhao C, Li Y, Peng Y, Xi F, Yang G (2018) Evodiamine promotes differentiation and inhibits proliferation of C2C12 muscle cells. Int J Mol Med 41(3):1627–1634